JOURNAL OF Materials CHEMISTRY

Magnetic susceptibility and crystal structure of the new oxovanadium phosphate $(NH_4)Zn(H_2O)(VO)_2(PO_4)_2(H_2PO_4)$

E. Le Fur,[a] O. Peña*[b] and J. Y. Pivan[a]

[a]*Institut de Chimie de Rennes, Laboratoire de Physicochimie, UPRES 1795-ENSCR, Ecole Nationale Supérieure de Chimie de Rennes, Campus de Beaulieu, Avenue du Général Leclerc, 35700 Rennes, France. E-mail: jean-yves.pivan@ensc-rennes.fr*
[b]*Laboratoire de Chimie du Solide et Inorganique Moléculaire, UMR 6511-CNRS, Campus de Beaulieu, Avenue du Général Leclerc, 35700 Rennes, France*

Received 15th June 2001, Accepted 8th October 2001
First published as an Advance Article on the web 19th November 2001

Intense blue powder samples of $(NH_4)Zn(H_2O)(VO)_2(PO_4)_2(H_2PO_4)$ were prepared in quantitative yield from hydrothermal treatments. $(NH_4)Zn(H_2O)(VO)_2(PO_4)_2(H_2PO_4)$ is monoclinic, space group $P2_1/n$ with parameters $a=10.7451(1)$ Å, $b=9.1941(1)$ Å, $c=13.2112(2)$ Å, $\beta=103.657(1)^\circ$, $Z=4$ ($R_1(F_o)=0.030$, $wR_2(F_o^2)=0.047$). The structure is based on linking of fused octahedra V_2O_9 with tetrahedra H_xPO_4 and $ZnO_3(H_2O)$. The remaining tunnels of the 3D framework $[Zn(H_2O)(VO)_2(PO_4)_2(H_2PO_4)]^-$ are occupied by the ammonium cations. The susceptibility data are consistent with the presence of dimers containing V^{4+} and small amounts of non-magnetic V^{5+} with strong antiferromagnetic coupling ($J\sim-29$ cm^{-1}).

Introduction

Since the discovery of the vanadium phosphorus oxides as efficient catalysts (nearly 20 years), very much attention has been devoted to the R–V–P–O system (R stands for neutral/cationic organic/inorganic species) that resulted in the synthesis of a constantly growing number of new solids with more or less intricate frameworks. Given what was known at the very beginning (especially for soft conditions such as hydrothermal techniques), the different research teams mainly reported about crystal data due to the difficulty in obtaining large amounts of pure solids. In turn with the exception of some very nice papers, the physical data were rather scarce. During the last decade, different routes have been investigated (high solid state, redox intercalation, hydrothermal treatments,...) that resulted in benchmark papers in which attempts to rationalise the synthesis procedures were proposed.[1–4] Nowadays, though the different mechanisms involved during the syntheses are not clearly understood,[5] the chemists can prepare in a reproducible way and quantitative yields pure solid RVPO's without detectable amounts of by-products.

Although all of these solids are based on linking of vanadium polyhedra (octahedra, pyramids) and phosphorus tetrahedra, the resulting frameworks are more or less intricate. The variability of the observed magnetic frameworks (isolated ions, pairs, chains, layers, *etc.*), the possibility for mixed or intermediate valence compounds containing V^{5+}, V^{4+} and(or) V^{3+}, and the super-exchange mechanisms through the phosphate bridges for the spin transfer between magnetic centres provide an exciting research area for the magnetochemists.

In this context, we report in this paper on the structure and the magnetic properties of $(NH_4)Zn(H_2O)(VO)_2(PO_4)_2(H_2PO_4)$. The susceptibility data are interpreted on the basis of an isotropic Heisenberg model for isolated dimers containing V^{4+} and small amounts of non-magnetic V^{5+}. Comparison is made with the related vanadyl hydrogen phosphate hemihydrate $VO(HPO_4)\cdot0.5H_2O$.[6]

Experimental

Synthesis

Mixtures of NH_4HCO_3 (0.180 g), V_2O_5 (0.154 g), Zn^0 (0.205 g, ships) were added to 5 ml of a solution of $\sim$2 M H_3PO_4, sealed in a 23 ml Teflon lined acid digestion bomb (Parr Instruments), then heated at 245 °C under autogenous pressure for 6 days. After slowly cooling to room temperature, the reaction products were filtered off, rinsed with distilled water and dried in air in a furnace maintained at 100 °C for 24 h. The reaction products were checked by visual examination under the microscope and appeared as pale blue platelet single crystals together with small amounts of well-shaped single crystals of the vanadyl hydrogen phosphate hemihydrate $VO(HPO_4)\cdot0.5H_2O$. These latter were separated manually from the bulk prior to subsequent analyses.

X-Ray diffraction

Single crystal studies were conducted at 300 K using an Enraf-Nonius diffractometer with graphite monochromated Mo Kα radiation ($\lambda=0.71073$ Å) equipped with a CCD detector that confirmed the X-ray powder diffraction analyses. During the experiment the goniometer and detector angular settings were optimised using the program COLLECT and the intensity data collection was performed in the ω–ϕ scanning mode.[7] The crystal to detector distance was 25 mm. The unit cell and the orientation matrix were refined using the entire data set of reflections. The diffraction spots were measured in full with a high accuracy as indicated by the statistical indicators ($\chi^2<1$) obtained from the program COLLECT.[7] Lorentz-polarization correction and peak integration were performed with DENZO and the data set was scaled using SCALEPACK.[7] The main crystallographic data and conditions for structure analysis are listed in Table 1 together with the reliability factors at the end of refinement. The systematic absences ($h0l$ $h+l=2n+1$, $0k0$ $k=2n+1$) indicate the

 DOI: 10.1039/b105271n

Table 1 Crystal data and summary of data collection, structure solution and refinement for $(NH_4)Zn(H_2O)(VO)_2(PO_4)_2(H_2PO_4)$

Empirical formula	$(NH_4)Zn(H_2O)(VO)_2(PO_4)_2(H_2PO_4)$
Color; habit	Blue; plates
Crystal system	Monoclinic
Space group	$P2_1/n$
Unit cell dimensions	$a=10.7451(2)$ Å
	$b=9.1941(1)$ Å
	$c=13.2112(2)$ Å
	$\beta=103.657(1)^\circ$
Volume	$V=1268.21(3)$ Å^3
Z	4
Formula weight	522.237 g mol^{-1}
Density (calc.)	2.735 g cm^{-3}
Data collection, structure solution and refinement	
Crystal size/mm^3	$0.5\times0.5\times0.09$
Absorption coefficient	37.9 cm^{-1}
Maximum 2θ	$2\theta\leqslant69.9^\circ$
Data collected	h: -17, $+16$
	k: 0, $+14$
	l: 0, $+21$
Unique data after merging	5330
Observed data ($>2.0\sigma(F^2)$)	3793
Free parameters	200
$R_{int.}$	0.032
Residuals R ($F^2>2.0\sigma(F^2)$)	0.030
wR	0.047
Extinction coefficient	0.28(2)
Min., max./e Å^{-3}	-0.54, $+0.78$
GooF	1.36

centrosymmetric space group $P2_1/n$. The starting structure model was extracted by direct methods using SIR97[8] and the refinements were made on F_o^2 with Jana2000.[9] The entire structure models (non-hydrogen atoms) were readily obtained from successive difference Fourier maps. At the end of refinement, anisotropic displacement parameters for non-hydrogen atoms and extinction coefficients were allowed to vary, resulting in the final residuals listed in Table 1. Hydrogen atoms were not located experimentally and were input, from electroneutrality requirements, in the final formula after accurate scrutiny of the framework counting the non-shared oxygen atoms around phosphorus and zinc. Atomic positional coordinates and atomic displacement parameters are given in Table 2. Selected bond distances and angles are listed in Table 3.

CCDC reference number 166367. See http://www.rsc.org/suppdata/jm/b1/b105271n/ for crystallographic data in CIF or other electronic format.

Table 2 Atomic coordinates and equivalent isotropic displacement coefficients U(eq.) (Å$^2\times100$) for $(NH_4)Zn(H_2O)(VO)_2(PO_4)_2(H_2PO_4)$

atoms	x	y	z	U(eq.)
V1	0.99293(2)	0.24491(2)	0.46859(1)	0.961(5)
V2	0.78878(2)	0.24912(2)	0.26355(1)	0.860(5)
Zn	0.63932(2)	0.24891(1)	0.52111(1)	1.499(5)
P1	0.72645(2)	0.49017(2)	0.07379(2)	0.824(7)
P2	0.78608(2)	0.50705(2)	0.43275(2)	0.789(7)
P3	0.60180(3)	0.33254(3)	0.74244(2)	1.310(8)
O1	0.86166(7)	0.38968(8)	0.38518(6)	1.04(2)
O2	0.64533(7)	0.60473(8)	0.11671(6)	1.17(2)
O3	0.80422(8)	0.40196(8)	0.16431(6)	1.38(2)
O4	0.70762(8)	0.59677(8)	0.34253(6)	1.40(2)
O5	0.64242(9)	0.25449(8)	0.26956(8)	2.01(2)
O6	0.51103(8)	0.26049(8)	0.79854(6)	1.19(2)
O7	0.88124(8)	0.59810(8)	0.51086(6)	1.53(2)
O8	0.63382(9)	0.39861(9)	0.99325(6)	1.71(2)
O9	0.69389(8)	0.43596(8)	0.48899(6)	1.66(2)
O10	0.82054(9)	0.56048(8)	0.01902(7)	1.91(2)
O11	0.9424(1)	0.24022(9)	0.57301(7)	2.22(3)
O12	0.72491(9)	0.3876(1)	0.82212(7)	2.45(2)
O13	0.6485(1)	0.2330(1)	0.66886(8)	2.67(3)
O14	0.53960(9)	0.4732(1)	0.68473(8)	3.04(3)
O15	0.4494(1)	0.2794(1)	0.4539(1)	5.19(5)
N	0.0574(1)	0.5434(1)	0.2662(1)	2.62(3)

Table 3 Selected bond lengths (Å), bond angles (°) with their standard deviations in brackets and bond valence sum values (Σs) for $(NH_4)Zn(H_2O)(VO)_2(PO_4)_2(H_2PO_4)$

		Distances	Angles				
V1	O11	1.598(1)					
	O7	1.952(1)	105.38(5)				
	O8	1.976(1)	104.05(5)	89.56(4)			
	O1	2.059(1)	98.62(4)	87.76(3)	157.06(4)		
	O2	2.085(1)	96.08(4)	156.03(4)	95.55(3)	78.45(3)	
	O6	2.301(1)	165.17(5)	86.35(3)	84.75(3)	72.35(3)	70.89(3)
Σs(V1) = 4.05							
V2	O5	1.594(1)					
	O3	1.955(1)	104.59(4)				
	O4	1.988(1)	103.92(4)	90.85(4)			
	O2	2.058(1)	98.40(5)	155.57(4)	91.54(3)		
	O1	2.067(1)	97.99(4)	89.74(3)	157.18(4)	78.89(3)	
	O6	2.324(1)	166.07(9)	85.12(3)	70.89(3)	70.84(3)	71.72(3)
Σs(V1) = 4.05							
P1	O2	1.557(1)					
	O3	1.521(1)	108.98(5)				
	O8	1.527(1)	107.33(5)	113.62(5)			
	O10	1.520(1)	112.23(5)	107.30(5)	107.47(5)		
Σs(P1) = 5.05							
P2	O1	1.568(1)					
	O4	1.529(1)	107.53(5)				
	O7	1.521(1)	108.77(5)	113.00(5)			
	O9	1.519(1)	111.04(5)	108.07(5)	108.45(5)		
Σs(P2) = 5.01							
P3	O6	1.510(1)					
	O12	1.567(1)	110.65(5)				
	O13	1.505(1)	113.73(5)	110.80(5)			
	O14	1.568(1)	110.47(5)	104.79(5)	110.88(5)		
Σs(P3) = 4.98							
Zn	O9	1.897(1)					
	O10	1.891(1)	131.66(4)				
	O13	1.937(1)	110.44(4)	104.63(4)			
	O15	2.044(1)	96.20(5)	105.92(5)	104.85(6)		
Σs(Zn) = 2.13							

Thermogravimetric measurements

Thermogravimetric analyses were performed using a SHIMADZU thermogravimetric analyser on crushed samples up to 900 K in flowing N_2 with a rate of 5 K min^{-1}. A continuous loss of weight ($\sim$8%) is observed up to 800 K that is attributed to dehydration and evolution of NH_3. After the heat treatments, the resulting product was recovered as a dark-green powder, the X-ray diffraction pattern of which is unknown.

Magnetic susceptibility studies

The susceptibility measurements were made on 124.5 mg of a powder sample that was zero-field cooled. The experiment was carried out at 0.5 T in the temperature range 5–300 K with a SQUID (SHE) magnetometer–susceptometer. With increasing temperature, the susceptibility first reaches a minimum at $T\sim12$ K, increases rapidly to a maximum at $T\sim50$ K then decreases smoothly with temperature. The negative deviation of the χT curve at lower temperature shows that the prevailing interactions are antiferromagnetic. The upturn on $\chi=f(T)$ curve at $T\leqslant12$ K is ascribed to small amounts of paramagnetic centres. The high temperature part of the reciprocal susceptibility *vs.* temperature is well fitted by a Curie–Weiss law $\chi=C/(T-\theta)$ with $\theta=-38.4$ K. From the fit of the Curie–Weiss law, the effective moment per V^{4+} ion $\mu_{exp}=1.68\ \mu_B$ is obtained that is almost identical to the value 1.73 μ_B expected for a $S=1/2$ ion. A good fit of the overall susceptibility data is obtained by considering isolated dimers with an isotropic

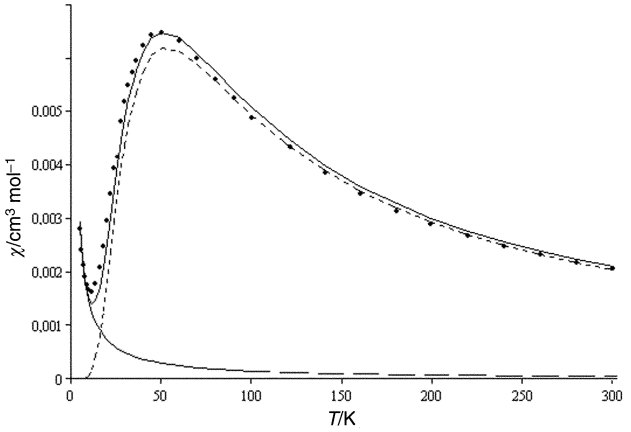

Fig. 1 Fit of the $\chi = f(T)$ curve for $(NH_4)Zn(H_2O)(VO)_2(PO_4)_2(H_2PO_4)$.

exchange interaction $H = -2Js_1.s_2$ using the Bleaney–Bowers equation.[10] The paramagnetic contribution at temperatures below 12 K is ascribed to small amounts of V^{5+} within the dimers. Isolated paramagnetic centers V^{4+} result that are assumed to follow Curie's law $\chi = C/T$ and the magnetic susceptibility takes the form $\chi = (1-x)\chi_{dim} + x\chi_{mono}$ where $\chi_{dim} = [g^2(3+\exp(-2J/kT))]/12T$, $\chi_{mono} = 3g^2/32T$ and x stands for the amount of isolated V^{4+}. The adjustable parameters were g, J and x and satisfactory results were obtained for $g = 1.94(5)$, $J = -29.3(2)$ cm^{-1} and $x = 0.044(2)$ as can be seen in Fig. 1.

Results

As shown in Fig. 2, the structure of $(NH_4)Zn(H_2O)(VO)_2(PO_4)_2(H_2PO_4)$ is formed by linking of V_2O_9 dimers with $Zn(H_2O)O_3$, PO_4 and H_2PO_4 tetrahedra leading to the formation of a three-dimensional framework. The asymmetric unit of the structure contains one zinc atom, two vanadium atoms, three phosphorus atoms, fifteen oxygen atoms and one nitrogen atom (Fig. 3). The two vanadiums are octahedrally coordinated to oxygen atoms with four equatorial bonds ($\bar{d}_{V\text{-}O} \sim 2.018$ Å), a typical vanadyl V=O bond at $d \sim 1.596$ Å and a longer *trans* V···O bond at $d \sim 2.313(2)$ Å. As usually found in oxovanadium chemistry, the oxygen atoms of the vanadyl group (namely O5 and O11) are not shared with other polyhedra. The VO_6 octahedra are part of dimeric unit V_2O_9 through face-sharing involving two equatorial oxygen atoms (O1 and O2) and the oxygen from the longer V···O bond that

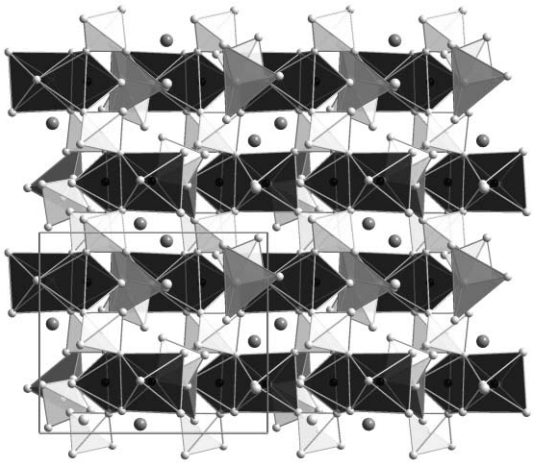

Fig. 2 View of $(NH_4)Zn(H_2O)(VO)_2(PO_4)_2(H_2PO_4)$ along the [001] direction. The black polyhedra are the VO_6 octahedra, the grey ones are the phosphorus and zinc tetrahedra. The unit cell is emphasized.

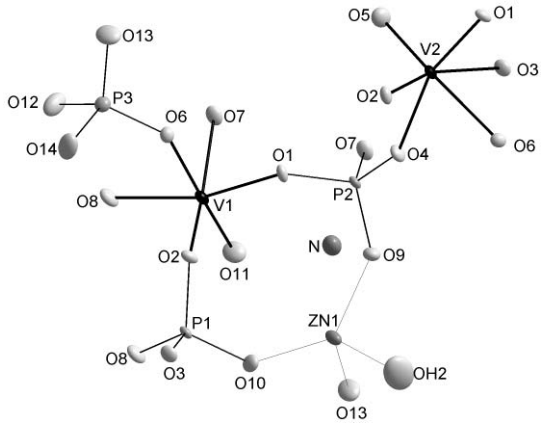

Fig. 3 View of the asymmetric unit of $(NH_4)Zn(H_2O)(VO)_2(PO_4)_2(H_2PO_4)$ (Ortep-style) showing the connectivity. Thermal ellipsoïds are at the 95% probability level.

results in a short V–V bond distance $d_{V\text{-}V} \sim 3.06$ Å. The dimers are corner connected to seven phosphate groups (six PO_4 and one H_2PO_4) through μ_2- and μ_3-oxo bridges. The oxygen atoms (O1, O2 and O6) from the common face of the dimer are those involved in the μ_3-oxo links. It is worth noting that smaller V–O–P bond angles occur at the μ_3-links ($126.56(4)^\circ \leqslant \alpha_{V\text{-}O\text{-}P} \leqslant 134.58(5)^\circ$) with respect to the V–O–P bond angles at the μ_2-links ($142.41(5)^\circ \leqslant \alpha_{V\text{-}O\text{-}P} \leqslant 146.50(5)^\circ$). Of the latter, the V–O–P bond angles involving the H_2PO_4 group are significantly increased. Though phosphate groups are present as PO_4 and H_2PO_4 in the structure, their polyhedra do not reveal appreciable differences. Indeed, the average values of P–O bond lengths $d_{av} = [P1\text{–}O] = 1.531(6)$ Å; $d_{av} = [P2\text{–}O] = 1.534(6)$ Å; $d_{av} = [P3\text{–}O] = 1.538(6)$ Å and O–P–O bond angles O–P1–O = 109.5(5)°; O–P2–O = 109.5(5)°; O–P3–O = 110.2(5)° are in good agreement with known values for orthophosphate species. Furthermore, with the exception of the bond P3–O6 ($d_{P\text{-}O} = 1.510(1)$ Å), it is worth noting that the oxygen atoms O1, O2 and O6 at the μ_3-oxo bridges are making the longer bond lengths for the different polyhedra. Additional connectivity is ensured through the corner-sharing (μ_2-links) of the phosphate groups to tetrahedral zinc atoms with P–O–Zn bond angles ranging from 131.27(5)° to 140.45(5)°. Only three oxygen atoms around Zn are linked to the phosphate groups, the fourth oxygen is very likely part of a water molecule. Appreciable deviations from the tetrahedral geometry occur around the zinc atoms. The Zn–O bond lengths range from 1.891(1) Å to 2.044(1) Å while the intra-polyhedral angles O–Zn–O vary between 96.2(1)° and 131.7(1)°. This has to be ascribed to a large extent to the inhomogeneous near neighbours of the zinc atoms which consist of two PO_4, one H_2PO_4 and one water molecule. From the preceding, the negatively charged 3D framework $[Zn(H_2O)(VO)_2(PO_4)_2(H_2PO_4)]^-$ results and tunnels develop along the [001] direction with rectangular cross-section of approximate area 2×3 Å^2 that are displaced from each other by half a translation along a and along b (Fig. 2). One half of the tunnels are covered with terminal OH groups of the H_2PO_4 in an ordered manner, the other half are occupied by the ammonium cations. These latter are surrounded by eight oxygen atoms at distances ranging from 2.850(1) Å to 3.233(1) Å. At last, bond valence sum calculations[11] give formal oxidation states in good agreement with the expected values for V^{4+} ($\Sigma s = 4.05, 4.05$), P^{5+} ($\Sigma s = 5.05, 5.01$ and 4.98) and Zn^{2+} ($\Sigma s = 2.13$).

Discussion

The overall topology of $(NH_4)Zn(H_2O)(VO)_2(PO_4)_2(H_2PO_4)$ resembles to a large extent that of the vanadyl hydrogen phosphate hemihydrate $VO(HPO_4)\cdot 0.5H_2O$,[6] the structure of

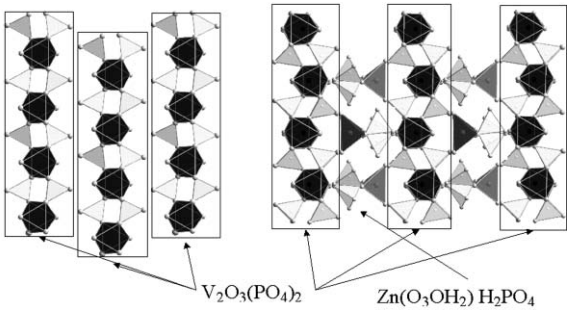

Fig. 4 Crystal chemical relationships between $(NH_4)Zn(H_2O)(VO)_2(PO_4)_2(H_2PO_4)$ and $VO(HPO_4)\cdot 0.5H_2O$.

which has been thoroughly described elsewhere. $VO(HPO_4)\cdot 0.5H_2O$ is a layered compound where V_2O_9 dimers are corner-connected throughout the structure to six hydrogenphosphate groups HPO_4. In turn, the phosphate groups link together three dimers *via* two μ_2- and one μ_3-oxo bridge, the latter non-shared oxygen being a terminal OH. The V_2O_9 dimers result from the face-sharing of octahedra $[V(H_2O)O_4]$, the water molecule and two equatorial oxygen atoms making the common face. The layers are held together through strong hydrogen bonds between the coordinated water molecule and the P–OH groups. Similar layered building units appear in $(NH_4)Zn(H_2O)(VO)_2(PO_4)_2(H_2PO_4)$ (dimers connected to six orthophosphate groups PO_4) with additional μ_2- and μ_3-oxo bridges involving interlayer $[H_2PO_4]$ and $[ZnO_3(H_2O)]$ groups. These supplementary groups connect the layers together and the three-dimensional topology results. Consequently, the V/P ratio differs for the two structures: V/P = 1 for $VO(HPO_4)\cdot 0.5H_2O$ while V/P = 2/3 for $(NH_4)Zn(H_2O)(VO)_2(PO_4)_2(H_2PO_4)$. Schematic relationships between the two structures are depicted in Fig. 4.

According to the benchmark paper by Roca *et al.*,[4] the topological parameters of the phosphate bridges govern the magnitude of the magnetic exchange coupling for oxovanadium phosphates. For the two structures we are dealing with, the only effective magnetic exchange pathways are di-μ-$(O,O')PO_4$ (μ_2-links) and di-μ-$(O)PO_4$ bridges (μ_3-links) (Fig. 5) and accordingly, one might expect the magnetic behaviour of $(NH_4)Zn(H_2O)(VO)_2(PO_4)_2(H_2PO_4)$ and $VO(HPO_4)\cdot 0.5H_2O$ to be very close. After Roca, the most active path is the di-μ-$(O)PO_4$ bridge and the susceptibility data are well analyzed in terms of isolated V2 dimers. As expected, the exchange parameter for $(NH_4)Zn(H_2O)(VO)_2(PO_4)_2(H_2PO_4)$ ($J = -29.3(2)$ cm^{-1}) compares satisfactorily with that obtained for $VO(HPO_4)\cdot 0.5H_2O$ ($J = -30.6$ cm^{-1}).[12] It is worth noting that the best fit of the susceptibility data was obtained considering small amounts of paramagnetic impurities as previously reported for $VO(HPO_4)\cdot 0.5H_2O$ and $VO(HPO_4)\cdot 2H_2O$.[13] This peculiar feature is seemingly an intrinsic property of these compounds and it appears reasonable that slight deficiency of hydrogen atoms occurs to counterbalance the additional V^{5+} centres for all of these structures. Accordingly, the formula $(NH_4)Zn(H_2O)(V^{IV}_{(1-x)}V^{V}_{x}O)_2(PO_4)_2(H_{2-x}PO_4)$ with $x \sim 4.5\%$ is more likely for the title compound.

Conclusion

The new $(NH_4)Zn(H_2O)(VO)_2(PO_4)_2(H_2PO_4)$ has been prepared in quantitative yield under hydrothermal conditions. The compound crystallizes in the monoclinic symmetry space group $P2_1/n$. The crystal structure is three-dimensional and shows structural similarities with $VO(HPO_4)\cdot 0.5H_2O$. The overall topology results from the heterocondensation of face-shared octahedra $[V_2O_9]$ with tetrahedra $[Zn(H_2O)O_3]$ and phosphate units $[H_2PO_4]$ and $[PO_4]$. The susceptibility data are consistent with the presence of isolated dimers coupled antiferromagnetically ($J \sim -30$ cm^{-1}). Small amounts of V^{5+} inside the dimers are responsible for the paramagnetic tail at the lowest temperature ($T < 12$ K).

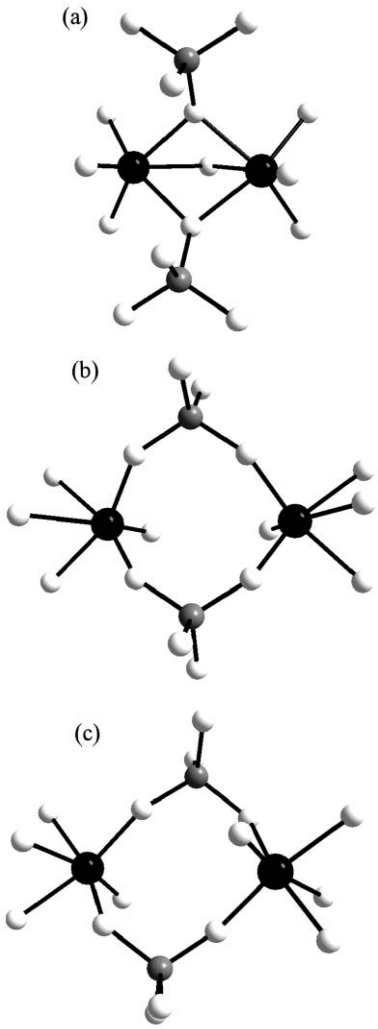

Fig. 5 The different active exchange pathways di-μ-$(O)PO_4$ (a) and di-μ-$(O,O')PO_4$ (b and c) that are present in $(NH_4)Zn(H_2O)(VO)_2(PO_4)_2(H_2PO_4)$.

Acknowledgement

The authors are indebted to Dr T. Roisnel for the single crystal intensity data collection on the Kappa CCD diffractometer (Université de Rennes I, LCSIM, UMR 6511).

References

1 G. Centi, F. Trifiro, J. R. Ebrer and V. M. Franchetti, *Chem. Rev.*, 1988, **88**, 55.
2 D. Beltrán-Porter, A. Beltrán-Porter, P. Amorós, R. Ibañez, E. Martinez, A. Le Bail, G. Ferey and G. Villeneuve, *Eur. J. Solid State Inorg. Chem.*, 1991, **28**, 131.
3 M. Roca, M. D. Marcos, P. Amorós, J. Alamo, A. Beltrán-Porter and D. Beltrán-Porter, *Inorg. Chem.*, 1997, **36**, 3414.
4 M. Roca, P. Amorós, J. Cano, M. D. Marcos, J. Alamo, A. Beltrán-Porter and D. Beltrán-Porter, *Inorg. Chem.*, 1998, **37**, 3167.
5 P. Amorós, M. D. Marcos, A. Beltrán-Porter and D. Beltrán-Porter, *Curr. Opin. Solid State Mater. Sci.*, 1999, **4**, 123 and references therein.
6 C. C. Torardi and J. C. Calabrese, *Inorg. Chem.*, 1984, **23**, 1308; M. E. Leonowicz, J. W. Johnson, J. F. Brody, H. Shannon and J. M. Newsam, *J. Solid State Chem.*, 1985, **56**, 370.
7 COLLECT, DENZO, SCALEPACK, SORTAV, Kappa CCD Program Package, Nonius BV, Delft, The Netherlands, 1998.
8 A. Altomare, M. C. Burla, M. Camalli, G. L. Cascarano,

C. Giacovazzo, A. Guagliardi, A. G. G. Moliterni, G. Polidori and R. Spagna, *J. Appl. Crystallogr.*, 1999, **32**, 115.
9 V. Petricek and M. Dusek, Jana2000: Crystallographic computing system for ordinary and modulated structures, *J. Appl. Crystallogr.*, 2001, **34**, 398, available free at http://www-xray.fzu.cz/jana/jana.html
10 D. Bleaney and K. D. Bowers, *Proc. R. Soc. London, Ser. A*, 1952, **214**, 451.
11 I. D. Brown and D. Altermatt, *Acta Crystallogr., Sect. B*, 1985, **41**, 244.
12 J. W. Johnson, D. C. Johnston, A. J. Jacobson and J. F. Brody, *J. Am. Chem. Soc.*, 1984, **106**, 8123.
13 G. Vileneuve, K. S. Suh, P. Amorós, N. Casañ-Pastor and D. Beltran-Porter, *Chem. Mater.*, 1992, **4**, 108.